SYNTHESIS AND CHARACTERIZATION OF ULTRAFINE-GRAIN TITANIA STABILIZED ZIRCONIA CUM ALUMINA COMPOSITES

By

M. MUSHTAQ AHMED

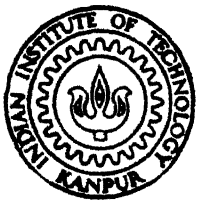

INTERDISCIPLINARY PROGRAMME IN MATERIALS SCIENCE

INDIAN INSTITUTE OF TECHNOLOGY, KANPUR

JULY, 1988

SYNTHESIS AND CHARACTERIZATION OF ULTRAFINE-GRAIN TITANIA STABILIZED ZIRCONIA CUM ALUMINA COMPOSITES

A Thesis Submitted
In Partial Fulfilment of the Requirements
for the Degree of

MASTER OF TECHNOLOGY

By

M. MUSHTAQ AHMED

to the

INTERDISCIPLINARY PROGRAMME IN MATERIALS SCIENCE
INDIAN INSTITUTE OF TECHNOLOGY, KANPUR

JULY, 1988

CERTIFICATE

This is to certify that the present work entitled " Synthesis and Characterization of Ultrafine-Grain Titania-Stabilized-Zirconia Cum Alumina Composites" by Mr. M. Mushtaq Ahmed has been carried out under my supervision and that it has not been submitted elsewhere for a degree.

July 27, 1988

(K.N. Rai)
Professor
Materials Science and
Metallurgical Engineering
Indian Institute of Technology
KANPUR

ACKNOWLEDGEMENT

I wish to express my profound sense of gratitude to Prof. K.N. Rai for his guidance, co-operation and encouragement during this work as well as throughout my M.Tech. programme.

I am grateful to Dr. D.C. Agrawal for his valuable suggestions and to Dr. Jitendra Kumar for his wholehearted help in carrying out electron microscopy studies.

I also express my sincere thanks to all the staff members of A.C.M.S. especially Mr. B. Sharma, Mr. B.K. Jain, Mr. Uma Shankar and Mr. Prasad.

I also wish to express my heartfelt appreciation of the help and co-operation provided by all my friends particularly Uniyal, Anup Sujoy, Saini, Adil, Mazumdar etc.

Thanks are also due, to Mr. Jawar Singh, for his prompt and excellent typing of this manuscript.

MUSHTAQ

CONTENTS

ABSTRACT

A literature survey of Phase Transformation Toughening has been conducted and a review has been presented. With the aim of fabricating Titania-Stabilized Zirconia (TSZ) Cum Alumina Composites, TSZ powders having the following compositions have been synthesized by co-precipitation : 15 mole % TiO_2-85mol% ZrO_2, 30 mole % TiO_2 - 70 mole % ZrO_2. Their grain growth kinetics and tetragonal phase stabilization have been evaluated by x-ray diffraction techniques. The TSZ powder having 15 mole % TiO_2 has been selected for fabricating the Zirconia Toughened Alumina (ZTA) composites. The ZTA composites with compositions varying from 2 vol. % to 100 vol. % TSZ have been sintered at 1600°C for 3 hours. These composites have been used for all further investigations. The density, porosity, tetragonal-phase retention, flexural strength, Young's modulus, Vickers hardness and fracture toughness have been evaluated.

CHAPTER - 1

INTRODUCTION

Basic theory; Fracture toughness improvement by stress induced phase transformation, Factors influencing the phase transformation; Theory of the present work, Possible applications.

There has been substantial work with reference to fundamental research and application on the polymorphic nature of zirconia and associated phase transformations. Pure zirconia has three well defined polymorphs viz., Monoclinic, Tetragonal and Cubic. The monoclinic form is the stable form at room temperature. Cubic zirconia is stable above 2370°C [1]. On heating, monoclinic zirconia transforms into tetragonal form over the temperature range of 1100-1200°C [1]. On cooling, the reverse transformation begins at 1200°C and proceeds over a temperature range of 1200 to 600°C until the transformation is complete [2]. This transformation from the tetragonal phase to the monoclinic phase involves a large shear strain ($\sim$ 8 %) and is accompanied by substantial volume increase (3 to 5 %) [3]. Furthermore, the transformation has two modes of induction i.e. it can be (i) stress induced and (ii) thermally induced.

The stress induced phase transformation is made use of in improving the fracture toughness of structural ceramics based on zirconia. The enhancement of fracture toughness in zirconia-toughened ceramics can be understood as follows :

Let us consider a composite ceramic body as shown in Fig. I.1 (a), in which particles of tetragonal - zirconia (t-ZrO_2) are dispersed in a matrix of another ceramic material whose fracture toughness is to be improved and whose modulus of normal elasticity is higher than that of zirconia. Now, if a sufficient tensile stress σ_c, is applied, as shown in Fig. I.1 (b), so as to propagate a crack through the material, the advancing crack-front tries to transect a t-ZrO_2 particle at some stage of its propagation, thereby exerting a tensile stress on it. When the strain energy of the t-ZrO_2 inclusion exceeds the tetragonal to monoclinic phase transition free energy, the crack tip exhausts its energy into transforming t-ZrO_2 into monoclinic state. This transformation results in a volume increase. Consequently, the t-ZrO_2 inclusion, during transition, tries to expand in the constricted space within the high modulus matrix material. The expansion of the zirconia particle in its constricted space is restricted by the high modulus matrix material surrounding it. As a result, the inclusion is subjected to a compressive stress, due to the transformation action. This tries to close-up the propagating crack. Thus the stress required to propagate the crack in the same direction is increased. Moreover part of the energy required to propagate the crack is also used up in t-ZrO_2 to monoclinic transition process. As a result the crack deviates to some other direction. This also results in crack branching.

It implies that there must exist ZrO_2 particles in fully or partially tetragonal state if the fraction toughness of the ceramic

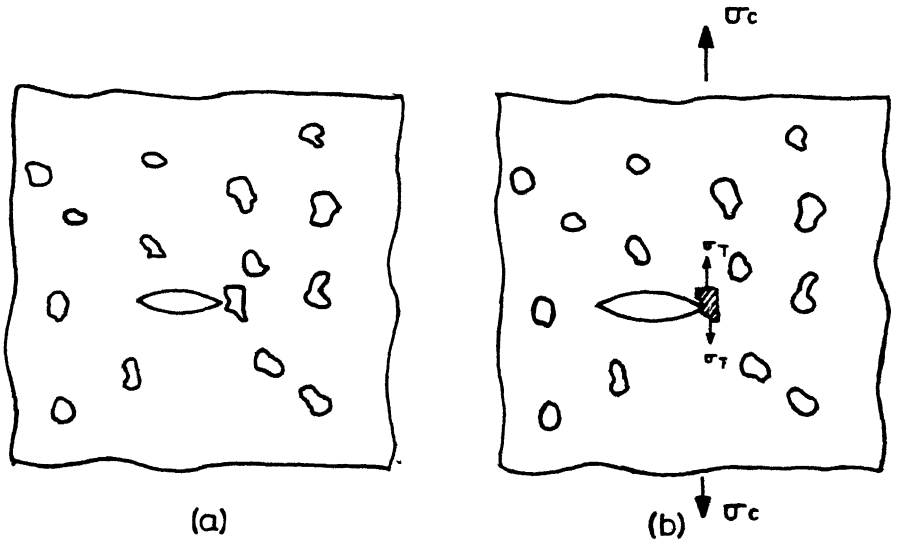

Fig I.1 Schematic Representation of the Interaction of a Pre existing Crack, being Propagated Through the Material, with a T ZrO_2 Inclusion

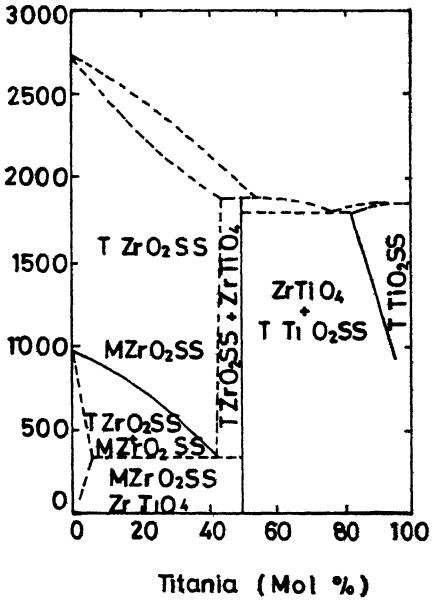

Fig. I.2 Phase Diagram of the System TiO_2-ZrO_2 Reproduced from "Oxide Ceramics" Physical Chemistry and Technology (Academic press, 1960)

composite is to be increased.

The retention of t-ZrO_2 in a partially stabilized state, at room temperature is dependent on the following factors :

1. Inclusion Size :

Through a thermodynamic analysis Lange [4] has shown that a critical inclusion size exists below which tetragonal phase retention is possible and above which it is not. For pure zirconia this critical inclusion size has been found to be 300 Angstroms.

2. Elastic Constraint [5] :

Elastic constraint on the t-ZrO_2 inclusion lowers the transformation temperature, thereby aiding retention.

3. Alloying Additions [5] :

Materials such as Y_2O_3, CaO, MgO etc. are known to lower the tetragonal to monoclinic (t-m) transformation temperature by reducing the transformation free energy. The addition of these materials is thus found to aid the retention of t-ZrO_2.

In the present investigation, all the above mentioned factors have been monitored to the advantage of t-phase retention. Titania was chosen as the alloying addition in order to stabilize t-ZrO_2, firstly, because titania lowers the t→m transformation temperature to the lowest level of 310°C [6,7] as shown in Fig. I.2 and secondly, because the co-efficient of thermal expansion of titania ($6.73 \times 10^{-6} m/^{\circ}C$) matches well with the co-efficient of thermal expansion of t-ZrO_2

(7.2×10^{-6} m/°C) and alumina (6.2×10^{-6} m/°C) [8]. The method of co-precipitation followed by thermal decomposition, employed in the present work, is known to produce ultrafine-grain powders [9] Alumina has a high modulus of normal elasticity (380.5 GN/m^2) which is two times the modulus of t-ZrO_2 (185.2 GN/m^2) [8]. It has therefore been selected in order to provide substantial elastic constraint.

Despite improved mechanical strength of zirconia composites fabricated by hot pressing, the fracture toughness has been found to degrade, by earlier workers [10]. It was therefore thought essential to investigate composites fabricated by sintering of ultrafine powders with alumina.

From the application perspective of ZTA composites, it has been predicted that owing to its very high hardness, alumina can have a profound impact on the area of cutting tool materials, provided the fracture toughness is improved [11]. E.D. Whitney [12] has predicted that the improved fracture toughness of ZTA composites makes them a very attractive insert for taking roughing operations on refractory metals where conventional ceramics connot be applied. Some of the present applications of sintered alumina are : As materials for guiding nozzles in automatic lathes, steel wear rings in pumps, grinding wheels, spark plug insulators etc. [13]. An increase in fracture toughness of sintered alumina through incorporation of t-ZrO_2 makes it more appealing for all the above applications.

OBJECTIVES OF INVESTIGATION

1. To synthesize ultrafine-grain size Titania Stabilized Zirconia (TSZ) in the tetragonal form.

2. To study the kinetics of grain growth and retention of tetragonal phase with reference to firing time, temperature and percentage titania content in TSZ powder.

3. To fabricate zirconia Toughened Alumina Composites using the TSZ powder and to evaluate their grain growth kinetics, phase (TSZ) retention and mechanical properties.

--

CHAPTER - 2

EXPERIMENTAL PROCEDURE

Starting materials; Synthesis of titania-stabilized-zirconia (TSZ) powder; Preparation of zirconia-toughened-alumina (ZTA) composites; Characterization of TSZ powder; Characterization of TSZ cum alumina composites.

2.1 Starting Materials :

The powders used for making the green compacts were Alumina and Ultrafine TSZ powder. Alumina powder having a purity of 99.07% and a particle size of -100 mesh was obtained from Sisco Research Laboratories (Bombay). The TSZ powder was synthesized in the laboratory. The details of chemicals used for TSZ preparation are shown in the Table 2.1 below.

Table 2.1

Chemical	Morphologh	Chemical Grade	Purity	Manufacturer
1. Titania (TiO_2)	Tetragonal (Anatase)	A.R.	99.4 %	Glaxo Laboratories (Pvt.) Limited, Bombay
2. Zirconium Oxy-chloride ($ZrOCl_2 . 8H_2O$)	-	A.R.	99.3 %	Fisons, Philadelphia, U.S.A.
3. Sulphuric Acid (H_2SO_4)	-	A.R.	98.0 %	I.D.P.L., Hyderabad(India)
4. Ammonia Solution	-	A.R.	25%	S.D. Fine Chem. Pvt. Ltd. Boisar

2.1.1 Synthesis of TSZ Powder :

First, titanium disulfate* ($Ti(SO_4)_2$ was obtained by the action of hot sulfuric acid on titanium dioxide (TiO_2) [14]. The following equation represents this reaction [16] :

$$TiO_2 + 2H_2SO_4 \rightarrow Ti(SO_4)_2 + 2H_2O$$

Titania powder was slowly and thoroughly mixed with concentrated sulfuric acid, in the ratio 1 : 8 by weight, in a glass beaker. The purpose of the slow addition of titania powder was to avoid local overheating [14,15]. The beaker containing this mixture was gently heated with simultaneous stirring at regular intervals. Continuous stirring should be avoided because the titanic sulfate formed has a high tendency to decompose on coming into contact with even traces of moisture from the atmosphere. The sulfating reaction was carefully allowed to proceed at a temperature below the normal boiling point of sulfuric acid [15]. After cooling, the solution was diluted by continuously by adding ice water [16] from a pipette.

The titanic sulfate solution so obtained was standardized by gravimetric titration [19] by precipitating into hydroxide form using $NH_4(OH)$ solution followed by decomposition into TiO_2.

Aqueous solution of zirconium oxychloride was added to the standardized titanic sulfate solution to yield mixed hydroxide precipitates of the compositions : 15 mole % $Ti(OH)_4$ - 85 mole % $Ar(OH)_4$, 30 mole % $Ti(OH)_4$ - 70 mole % $Zr(OH)_4$ and 40 mole % $Ti(OH)_4$ - 60 mole % $Ti(OH)_4$ after slow co-precipitation with

* Also termed titanic sulfate

ammonium hydroxide, $NH_4(OH)$, in a large flask. This flask was placed on a magnetic stirrer and ammonia solution was slowly added from a burette with simultaneous and constant stirring. The flask was intermittently cooled by shutting off the burette and dipping it in ice water to avoid the formation of metatitanic acid [16]. The process was carried out till completion of the precipitation. The following equations represent the reactions taking place during the co-precipitation [16] :

$$Ti\ (SO_4)_2 + NH_4OH \rightarrow Ti(OH_4 + (NH_4)_2\ SO_4$$

$$ZrOCl_2 + NH_4OH \rightarrow Zr(OH)_4 + NH_4Cl$$

The co-precipitates were dried by gently warming [17] to avoid agglomeration. The co-precipitates were then ground in a mortar-pestle. This mixed hydroxide powder was then heated to different temperatures and the exact temperature of complete decomposition was determined for each of the three sets of powders, by x-ray diffraction technique of phase identification. On decomposing according to the following reactions [16], composite TSZ powder was obtained with zirconia in the tetragonal phase.

$$Ti\ (OH)_4 \rightarrow TiO_2 + 2H_2O$$

$$Zr\ (OH)_4 \rightarrow ZrO_2 + 2\ H_2O$$

2.2 Preparation of ZTA Composites :

The commercial alumina powder was first ground in an agate

centrifugal ball mill (Pulverizette, Fritsch, Germany) for ten hours using alumina milling medium and acetone as the vehicle. The slurry obtained after milling was dried thoroughly in an oven at 80°C. The TSZ powder, in calculated amounts, was weighed and mixed with dry alumina. Mixing was done, under the same conditions as for grinding, for $1\frac{1}{2}$ hours. The slurry was again dried. The powders obtained were compacted, in a hand operated hydraulic press at 30 M.Pa., in the form of pellets of size 2.4 cm x 1 cm x 0.4 cm. Zinc stearate was used as a lubricant. Aqueous solution of polyvinyl alcohol (PVA) (of strength 2 % by weight) was mixed with the TSZ-alumina powder in the ratio of 1 : 20 by weight, in order to provide adequate green strength. These compacts were dried at 150°C for a day, followed by sequential heating to 400°C, soaking at this temperature for one hour, attaining 1600°C and holding at this temperature for three hours. The rate of heating to 1600°C was kept at 100°C per hour, throughout the sintering operation. The cooling down to room temperature consisted of cooling from 1600°C to 1300°C in one hour, holding at 1300°C for one hour, cooling to 1000°C in one hour followed by furnace cooling after switching off the furnace. These ZTA pellets were used for all further study. Table II.2 gives the details of the ZTA lines.

2.3 Characterization :

The TSZ powderand the ZTA composites were analysed separately.

2.3.1 Characterization of TSZ powder :

Each of the three sets of TSZ powders was analysed for particle size distribution, grain size and phase stability.

TABLE II.2

COMPOSITIONS OF ZTA SERIES

No. of the Series	Volume % TSZ	Volume % Al_2O_3
ZTA 0	0	100
ZTA 1	2	98
ZTA 2	5	95
ZTA 3	10	90
ZTA 4	15	85
ZTA 5	25	75
ZTA 6	40	60
ZTA 7	50	50
ZTA 8	60	40
ZTA 9	70	30
ZTA10	80	20
ZTA11	90	10
ZTA12	100	0

(a) Determination of Particle Size Distribution:

The particle size distribution was determined with the help of Coulter Counter. The measurements were carried out under the following experimental conditions :

(i)	Aperture diameter	:	50 μm
(ii)	Manometer Volume	:	0.05 ml
(iii)	Gain Control		5
(iv)	Calibration factor,k	:	1.32
(v)	Matching Switch	:	10
(vi)	Electrolyte	:	NaCl
(vii)	Dispersant	:	Coulter

The number of particles in each particle size interval were noted and tabulated. Three runs were taken for each interval and the average number of counts was considered for representing the particle size distribution.

(b) Determination of the Average Grain Size :

The grain size determination of TSZ powders was carried out, by x-ray diffraction technique using Debye line broadening concept [32], with respect to three parameters- time, temperature and percentage titania content. During each grain size determination, one of the parameters was varied while the other two were kept constant. The x-ray diffraction patterns were obtained using a RICH-SEIFERT, ISO-DEBYE FLEX 200 2D diffractometer. The various parameters employed are given in Table : II.2. below :

Table II. 2

Experimental parameters used in x-ray diffraction analysis

Scanning speed	:	1.2°/ minute
Chart Speed	:	30 m.m./min.
Time Constant	:	10 seconds
Target	:	CuK (λ = 1.5405A°)
Filter	:	Nickel
Voltage/Current	:	30 kV/20mA
Beam Slit	:	2 mm.
DetertorSlit	:	0.3 m.m.

(c) Quantitative Phase Analysis by X-ray Diffraction :

The x-ray diffraction patterns obtained for particle size measurements were also used for determination of the retention of tetragonal phase by comparing intensities of tetragonal (III) and monoclinic ($II\bar{I}$) peaks as suggested by emperical relations developed by Evans et. al [17].

2.3.2 Characterization of ZTA Composites :

The ZTA composites were analysed for the grain growth kinetics, phase stability sintered density, true density, open porosity, closed porosity, true porosity, Vickers hardness, bend

strength, Young's modulus and fracture toughness, Kc.

(a) Grain growth kinetics and Phase Stability Determinations :

The procedure used here is identical to that used, for the analysis of these characteristics, in TSZ powder. The formula used for grain size determination was [27] :

$$\text{Average Grain Size} = \frac{0.9\lambda}{B \cos\theta}$$

where, λ = Wavelength of the radiation used

2θ = Peak position from the x-ray diffraction pattern

$B = \sqrt{B_M^2 - B_S^2}$ where B_M and B_S are the measured breadth at half maximum intensity of the line from the sample under consideration and the standard respectively.

(b) Determination of Sintered Density and Open Porosity [20] :

The moisture present in the samples was eliminated by heating them in an oven at 150°C for one day. Their dry weight, W_{air}, was taken on a SARTORIOUS-2006MP electronic balance. The samples were then immersed in a boiling water, bath for two hours. The bath was then allowed to cool and the weigh, W_{water}, of each sample immeresed in water was taken. The samples were then taken out, dabbed with tissue paper in order to remove enternal water, and their saturated weight, W_{sat}, was taken in air.

The following formulae were used in order to calculate the sintered density and open porosity :

$$\text{Sintered density (Ps)} = \frac{W_{air}}{W_{sat} - W_{water}}$$

$$\% \text{ Open porosity} = \frac{W_{sat} - W_{air}}{W_{sat} - W_{water}}$$

(c) True density and true porosity measurements :

The samples were ground to a fine powder so that they passed through a 100 mesh seive and dried in an oven at 150°C. The weight of a clean pycnometer was taken (W_1). The pycnometer was filled with enough sample so that it was slightly more than quarter full and its weight, W_2, was taken. The pycnometer was filled to one half of its volume with distilled water and boiled in a water bath for an hour. Then, the pycnometer was cooled, filled to the top with distilled water and the stopper was inserted. The weight, W_3, of the pycnometer and its contents was taken. The pycnometer was emptied of the sample, washed, dried, filled completely with distilled water and its weight, W_4, was taken. The following formulae were used in order to calculate the true density and true porosity values:

$$\text{Specific Gravity} = \frac{W_2 - W_1}{(W_2 - W_1) - (W_3 - W_4)}$$

$$\text{True density} = \text{Specific gravity} \times (d_w - d_a)$$

where, d_w and d_a are the densities of water and air respectively at the temperature at which the test was performed.

$$\% \text{ True porosity} = \left(1 - \frac{\text{sintered density}}{\text{True density}}\right) \times 100$$

$$\% \text{ Closed porosity} = \% \text{ True porosity} - \% \text{ open porosity}$$

(d) Vicker's hardness [22,23] :

The samples were polished initially by abrading successively on 0, 2/0, 3/0 and 4/0 grade emery papers using liquid paraffin lubricant and finally lapping on a polishing wheel covered with velvette cloth using 0.5 μm - alumina powder suspended in water as the abrasive.

Subsequently, indentations were carried out on a Vicker's Testing machine having a load range of 1 to 30 Kg. A load of 10 Kg. was used for the present investigation. The average length, L, of the diagonals was measured on a Omnicon Alpha 500 model image analyser manufactured by Baush and Lomb. The image analyser was used in conjunction with a Baush and Lomb microscope at a magnification of 100x. The Diamond pyramid Hardness number (DPH) was calculated using the following formula [27]

$$\text{DPH} = \frac{1.854P}{L^2}$$

From the DPH number values, the absolute hardness (in G.Pa) was obtained from the formula given by the empirical relation [28]:

$$H = \frac{\text{DPH}}{3}$$

(e) Flexural Strength [21]:

The flexural strength was determined by three-point-bending, on an Instron-1195 testing machine, as shown in Figure 2. below. The following experimental parameters were used for the three-point-bending test: span (L) = 1.8 cm

Width of the sample (b) = 0.6 cm

Depth of the sample (d) = 0.2 cm

Chart Speed = 0.05 mm/ minute

Strain rate = 50 m.m./ minute

Load cell used = 1000Kg (Maximum Limit)

The load (P) at fracture was determined in each case. Five samples were tested for each composition. The flexural strength was calculated from the expression [21]:

$$\text{Flexural Strength} = \frac{3}{2}\,\frac{PL}{bd^2}$$

where, D = load at fracture

L = Span

b = Width of the sample

d = depth of the sample

(f) Young's Modulus :

The load (L) at fracture obtained from the flexural strength test was used. In addition, the total central deflection Y_{ct} was determined from the load-deflection chart by multiplying

the crosshead speed with the time taken from the time of application of the load upto the time of incipience of bend fracture. The errors, in the measurement of the actual central deflection, due to deflections in the machine and fixture are eliminated by initially testing a "dummy" specimen [21] whose flexural rigidity EI is much larger than that of the actual specimen under the same experimental conditions as those used for the actual tests. After the "apparent" or total deflection, at failure, of the actual specimen is determined, the error due to deflection in the machine, jig etc. is eliminated by subtracting the deflection, measured during the "dummy" test, at the load corresponding to the actual load of fracture of the specimen under consideration. The dimensions of the dummy specimen used in the present investigations are :

Length (L) = 2.00 cm

Width (b) = 1.5 cm

Depth (d) = 0.3 cm

The following formula was used in the calculation of Young's modulus [21] :

$$E = \frac{11}{384} \frac{PL^3}{Y_C I}$$

where P = load at fracture

L = Span

Y_C = Central deflection

I = Second moment of area of the section about the neutral axis i.e., $\frac{bd^3}{\quad}$

(g) Fracture Toughness [22,23,24] :

The experimental procedure followed for fracture toughness determination is almost similar to that for flexural strength measurement except that, here, the indentation load is much higher (30Kg.) than that in the latter case. As a result of the use of a high indentation load, radial cracks are generated at the centre of the indentation. The crack length, $2C$, was measured two minutes after the indenter was removed [22,25]. The average length of the indentation diagonal was also measured in each case. The fracture toughness was calculated using the following emperical formula [22]:

$$\text{Fracture Toughness, } K_c = 0.016 \left(\frac{E}{H}\right)^{1/2} \left(\frac{P}{C^{3/2}}\right) \text{ M.Pa.m}^{1/2}$$

where E = Young's Modulus

H = Vicker's Hardness in absolute units

P = Indentation Load

2C = Radial Crack Length.

(h) Microstructure Analysis :

The samples were polished in the manner described in section 2.3.2 (e). The samples were then etched by immersing them in boiling phosphoric acid for one and a half hours [26]. A thin film coating of gold was then applied to the samples. These samples were used for metallographic studies by scanning electron microscopy on an ISI-60 Scanning Electron Microscope at 1000 magnification.

CHAPTER - 3

RESULTS AND DISCUSSION

Decomposition behaviour of the co-precipitate; Particle size analyses of the powders, Grain growth kinetics of the TSZ powder; Thermal stability of TSZ powder; Grain growth kinetics of ZTA composites, Thermal stability of ZTA composites; Open, Closed and True porosities, true and sintered densities; Vickers hardness; Bend strength, Young's modulus, and Fracture toughness of ZTA Composite series; Microstructure analysis of ZTA Composite Series.

3.1 Decomposition Behaviour of the Co-precipitated Hydroxide :

Figure III.3 shows the variation of the temperature of complete decomposition, of the co-precipitated hydroxide of zirconium and titanium [$Zr(OH)_4$ + Ti $(OH)_4$], as a function of the Ti $(OH)_4$ content. An observation of variation in the decomposition temperature is very important since it governs the initial grain size which is crucial in t-phase retention. The figure shows that upto a composition of (15 mole % $Ti(OH)_4$ - 85 mole% Zr $(OH)_4$), the decomposition temperature remains constant. A further increase in the $Ti(OH)_4$ content has a tendency to increase the decomposition temperature.

3.2 Particle Size Analysis :

The particle (which may consist of agglomerate of many grains ~~ground~~) size distribution for ground alumina and TSZ powder as analyzed by coulter counter method is shown in Table III.1

TABLE III. 1

Particle size distribution of ground alumina and TSZ powder

Size range microns	No. of particles falling in the size range	
	Al_2O_3	TSZ
0 - 0.564	12993	14817
0.564-0.711	13950	17462
0.711-0.896	18433	15464
0.896-1.12858	15700	14652
1.12858-1.422	8912	6542
1.422-1.792	5541	1449
1.792-2.257	2650	235
2.257-2.844	1949	745
2.844-3.583	904	367
3.583-4.514	263	43
4.514-5.688	212	235
5.688-7.166	309	302
7.166-9.0287	0	9
9.0287-11.375	0	3

Figure III.1 shows the histogram plot of particle distribution of ground alumina with the number of particle in various classes, expressed as fraction of the number of particles in that class in which the frequency is a maximum. The figure shows that the maximum

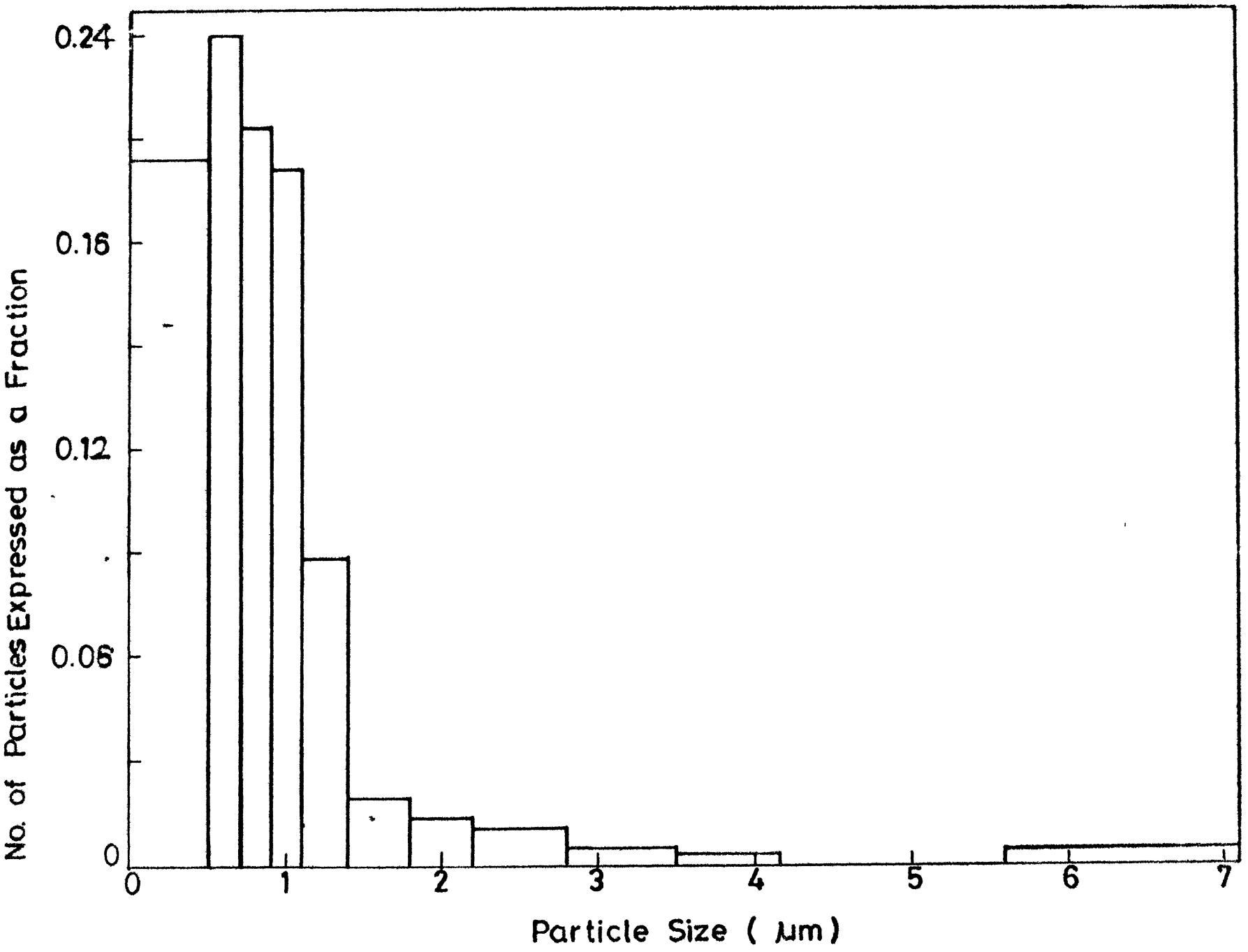

Fig. III.2 Particle Size Distribution of TSZ Powder.

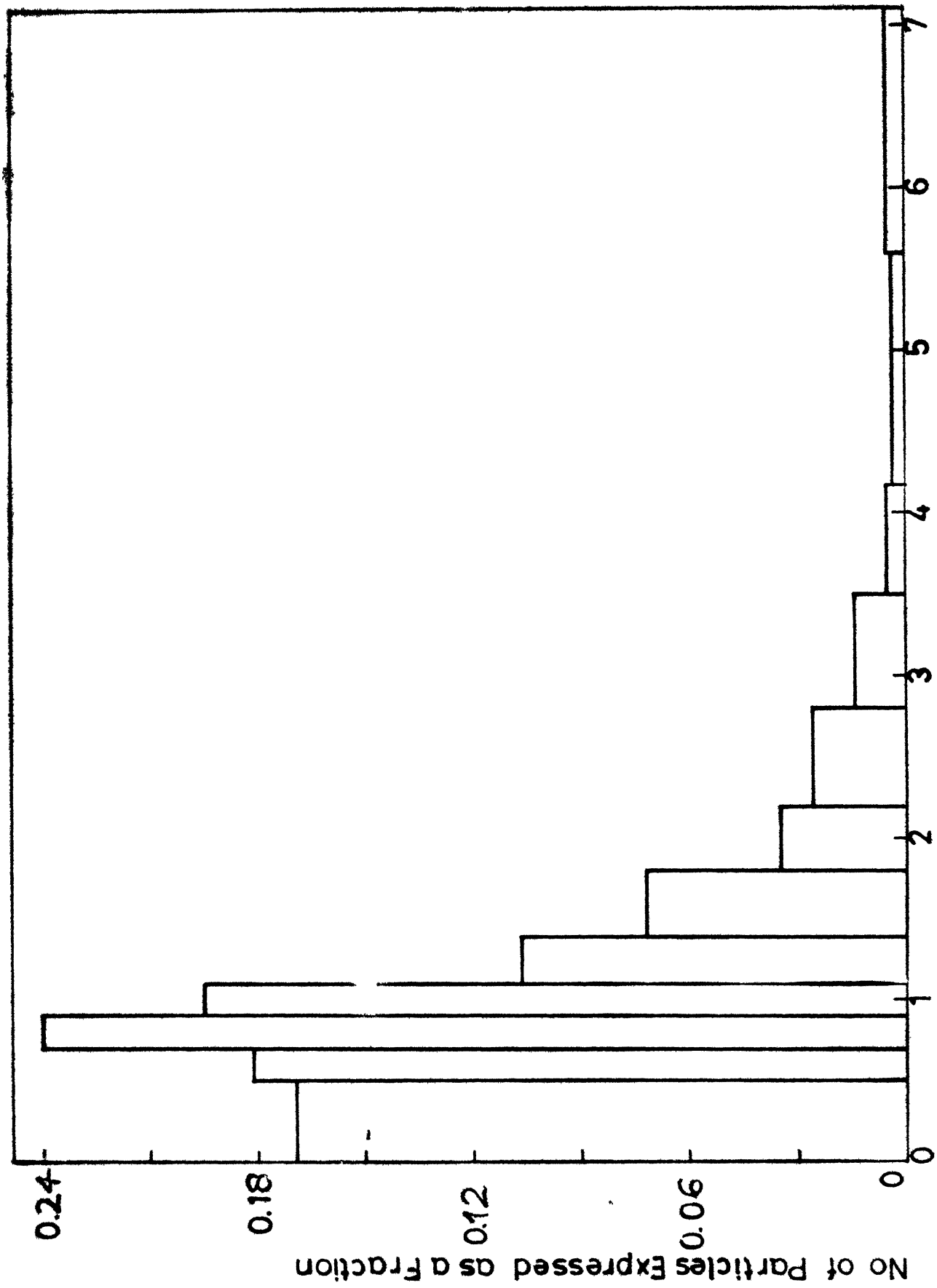

Fig.III.1 Particle Size Distribution of Ground Alumina.

frequency falls in the class (0.711 to 0.896) μm. The distribution is more or less symmetric on either sides of the maxima. This type of distribution is very much desirable in order to achieve optimum and uniform elastic constraint achieved due to efficient packing of the powder during compaction and sintering. Fig III.2 shows the histogram plot of TSZ powder. Here too, the particle size distribution is more or less similar to that of alumina. The maximum frequency here lies in the class range (0.564 to 0.711) μm, which is quite low. Thus the various measures (slow precipitation, rapid stirring during decomposition, gentle decomposition etc.) taken during synthesis have paid off.

3.3 Grain Growth Kinetics of TSZ Powder :

Figure III.4 shows a plot of average grain size (in Å) of the t-stablized titania-zirconia composite as a function of firing time of oxides. The data from which this figure was plotted is given in Table III.2. A study of the table and plot reveals three points of interest :

1. An increase in the time of firing initially causes the grain size to increase, as expected from the knowledge of normal grain growth kinetics, but beyond a certain time limit, in general, about 3 hours, the grain size starts decreasing. This is attributed to the gradual transformation of t-ZrO_2 into m-ZrO_2 as observed by X-ray diffraction for samples heat treated beyond certain length of time exhibiting appearance of m-phase.

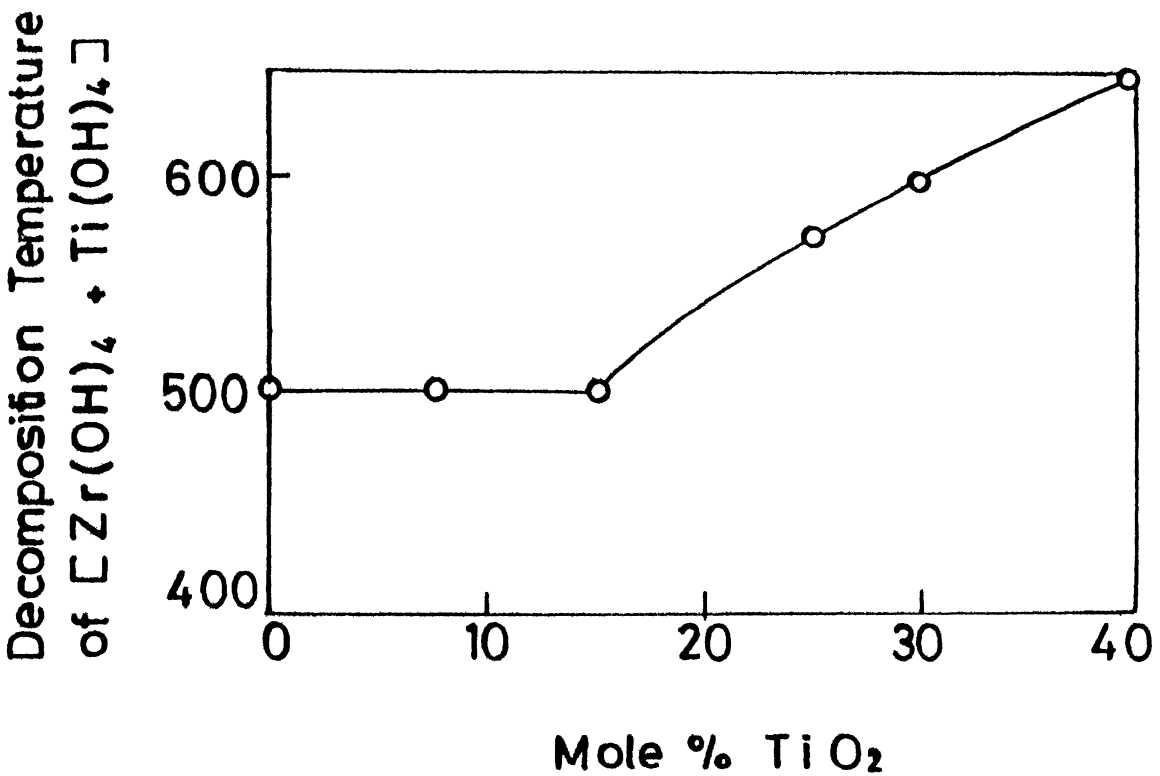

Fig. III.3 Decomposition Temperature of Co-precipitated Hydroxide [$Zr(OH)_4 + Ti(OH)_4$] as a Function of Mole % of TiO_2 or $Ti(OH)_4$.

TABLE : III.2

Composition (mole % TiO_2)	Temperature (°C)	Time (Sec.)	Grain Size (A°)
15	500°C	3600	110
,,	,,	7200	150
,,	,,	10800	179
,,	,,	14000	167
,,	600°C	3600	143
,,	,,	7200	200
,,	,,	10800	208
,,	,,	14000	182
,,	700	3600	180
,,	,,	7200	205
,,	,,	10800	219
,,	,,	14000	190
,,	1000	3600	210
,,	,,	7200	219
,,	,,	10800	223
,,	,,	14000	195
25	800	3600	112
,,	,,	7200	118
,,	,,	10800	130
,,	,,	14000	112
,,	1000	3600	155
,,	,,	7200	165
,,	,,	10800	185
,,	,,	14000	150

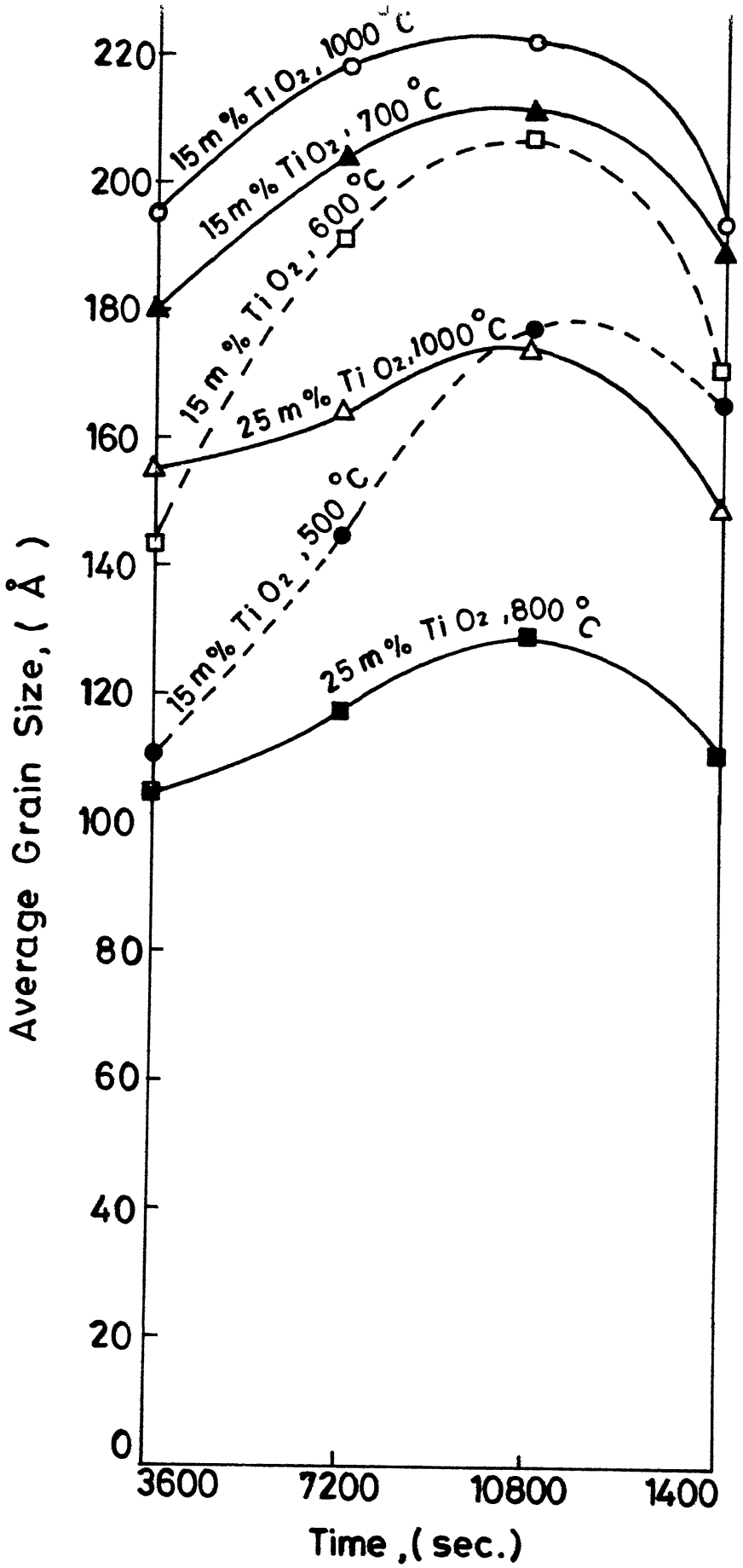

Fig. III. 4 Grain Size Dependence on the Firing Time of Composite (TSZ) Powder at Constant Temperatures and Constant Compositions.

2. An increase in the amount of titania tends to decrease the grain size and suppress grain growth rate. Thus titania is very important in t-phase retention by keeping the grain size below the critical limit.

3. An increase in temperature tends to increase the grain size with decreasing grain growth rate. This appears paradoxical. However it can be explained by invoking two competing processes i.e. (i) the enhance in grain growth with increasing time and temperature and (ii) decrease in t-phase grain size due to enhance rate of transformation with time and temperature. The later having more importance at elevated temperature. More clearly it can be said that a tetragonal particle is being consumed into monoclinic continuously resulting into gradual loss in particle size of the tetragonal phase.

Figure III.5 ~~which~~ is a plot of average grain size (in A·) versus soaking temperature (in °K). The following points can be noted from this graph.

1. The grain size goes on on increasing upto a certain temperature and then decrease. This is due to the transformation from tetgragonal to monoclinic phase, when the sample is heated behond the t-m transformation temperature.

2. The temperature at which the grain growth rate becomes negative (i.e. the t-m transformation temperature) increases with increase in titania content. This behaviour can again be attributed to the temperature, and gain size dependent phase transformation.

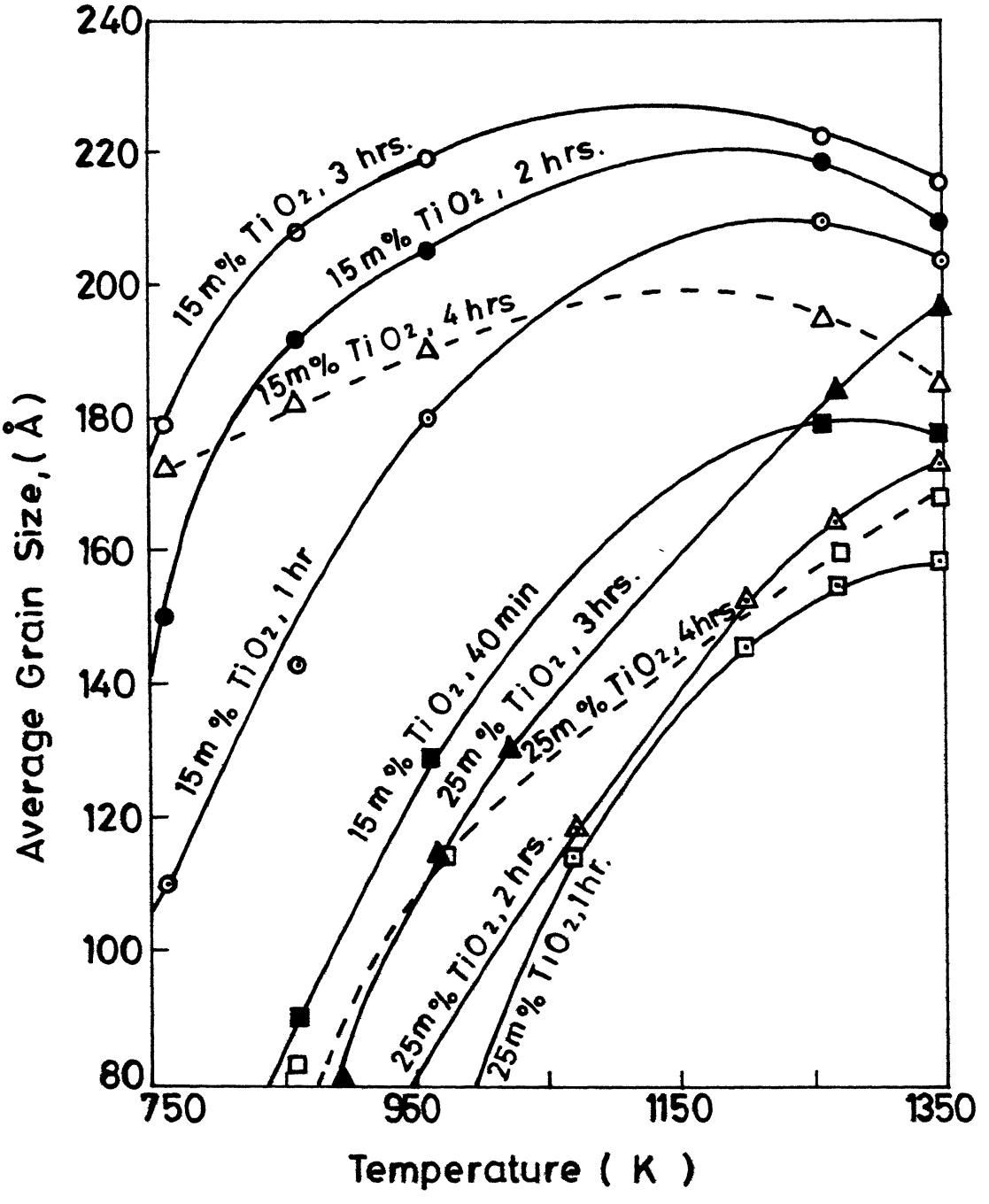

Fig.III.5 Temperature Dependence of Grain Diameter of (TSZ) Powder at Constant Compositions and Constant Time.

3.4 Thermal Stability of TSZ Powder :

Figure III.6 shows the variation of the percentage tetragonal phase content with increase in firing temperature of TSZ powder containing 15 mole% TiO_2. The firing time is kept constant at 2 hours. From the graph we can infer that the rate of decrease in tetragonal phase content with increasing temperature is lower at lower temperature ranges (500°C to 800°C) than at higher temperature ranges (800°C to 1000°C). This means that the effectiveness of the stabilizer in decreasing the chemical free energy change of the t-m transformation is lowered at higher temperatures. Figure III.7 shows the sequence of phases observed at room temperature in three series of zirconia powders which were initially in tetragonal phase. The figure shows that complete retention of the tetragonal phase is possible upto 680°C in pure unstabilized zirconia, upto 720°C in 15 mole% TiO_2 TSZ series and upto 800°C in 25 mole % TiO_2 TSZ series. Thus TiO_2 has a good stabilizing effect.

3.5 Variation of Grain Size with Vol. % TSZ in ZTA Composites :

Figure III.9 shows that, initially, the rate of grain growth, with Vol. % TSZ, is very high upto 25 vol. % TSZ then declines and finally becomes zero. This is expected due to a loss of elastic constraint because of a continuous decrease in the alumina content.

3.6 Thermal Stability of ZTA Composites :

Figure III.8 shows the variation of the percentage tetragonal

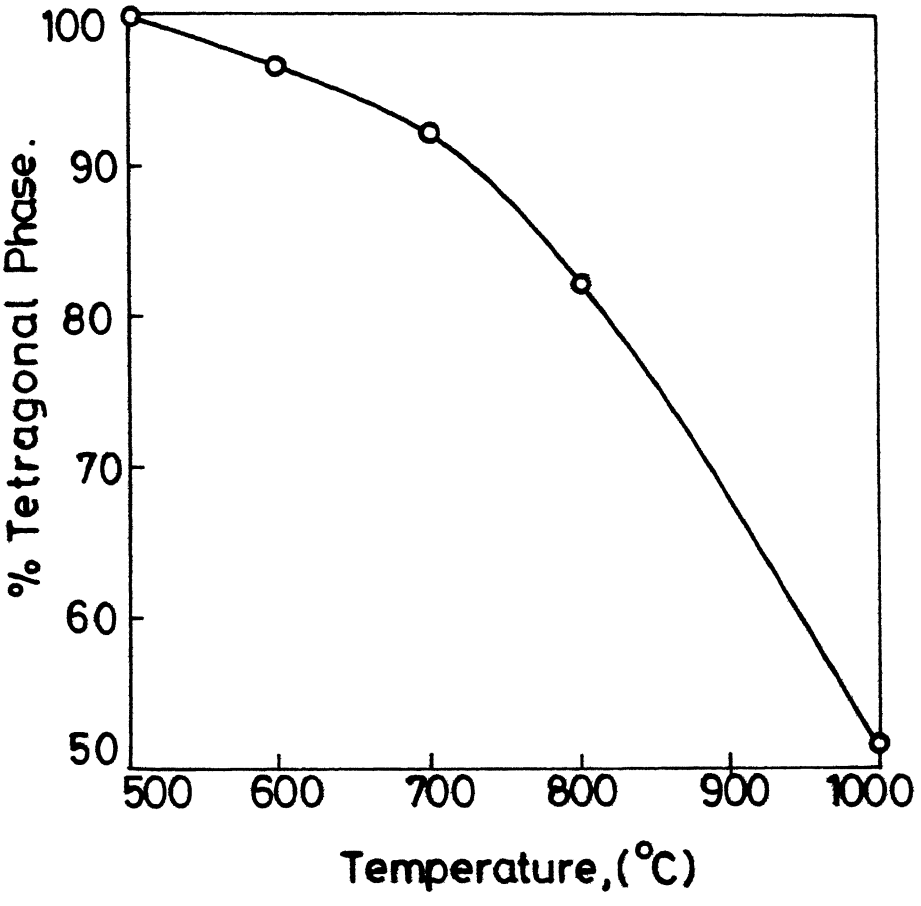

Fig.III.6 Tetragonal Monoclinic Transformation in TSZ Powder as a Function of Temperature.

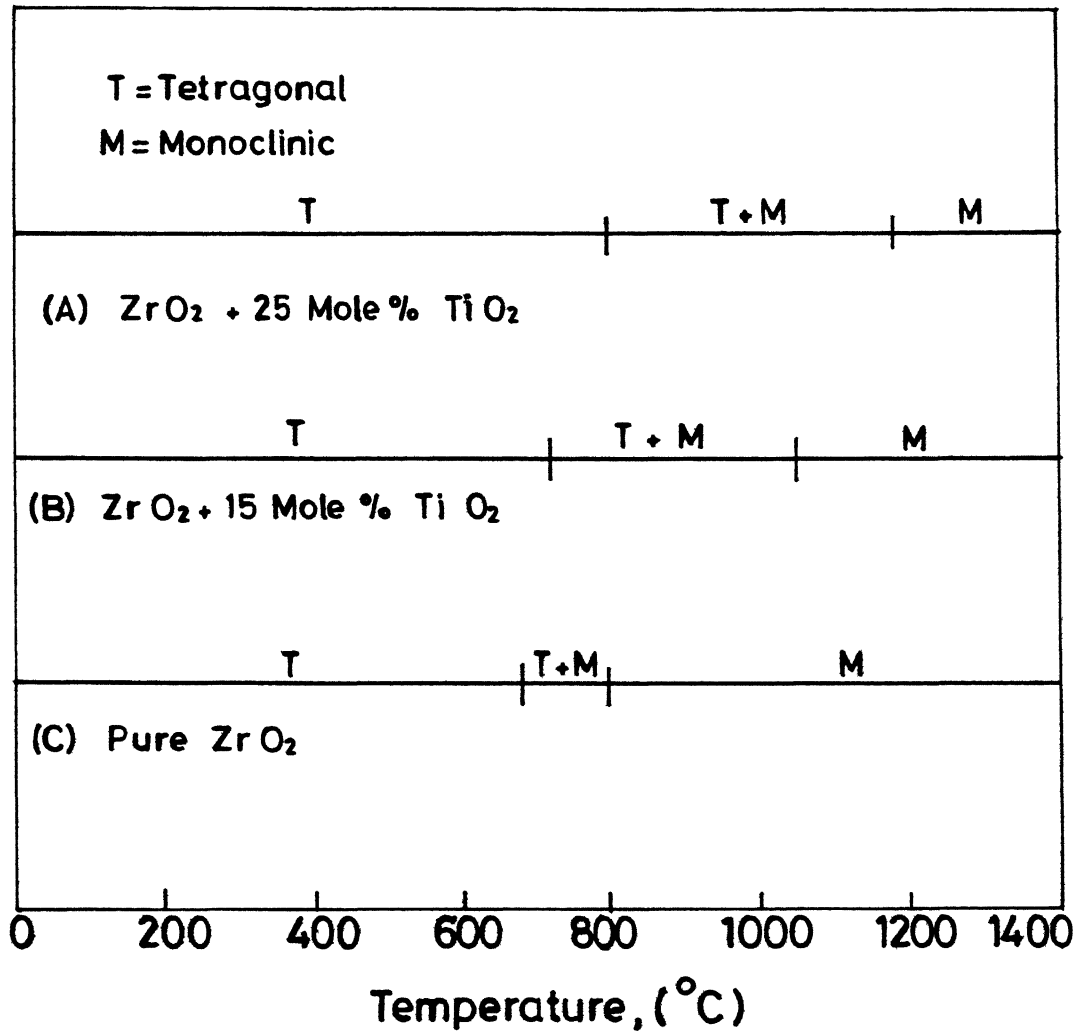

Fig.III.7 The Phases Present at Room Temperature in TSZ as Function of Thermal Shocking at Various Temperatures.

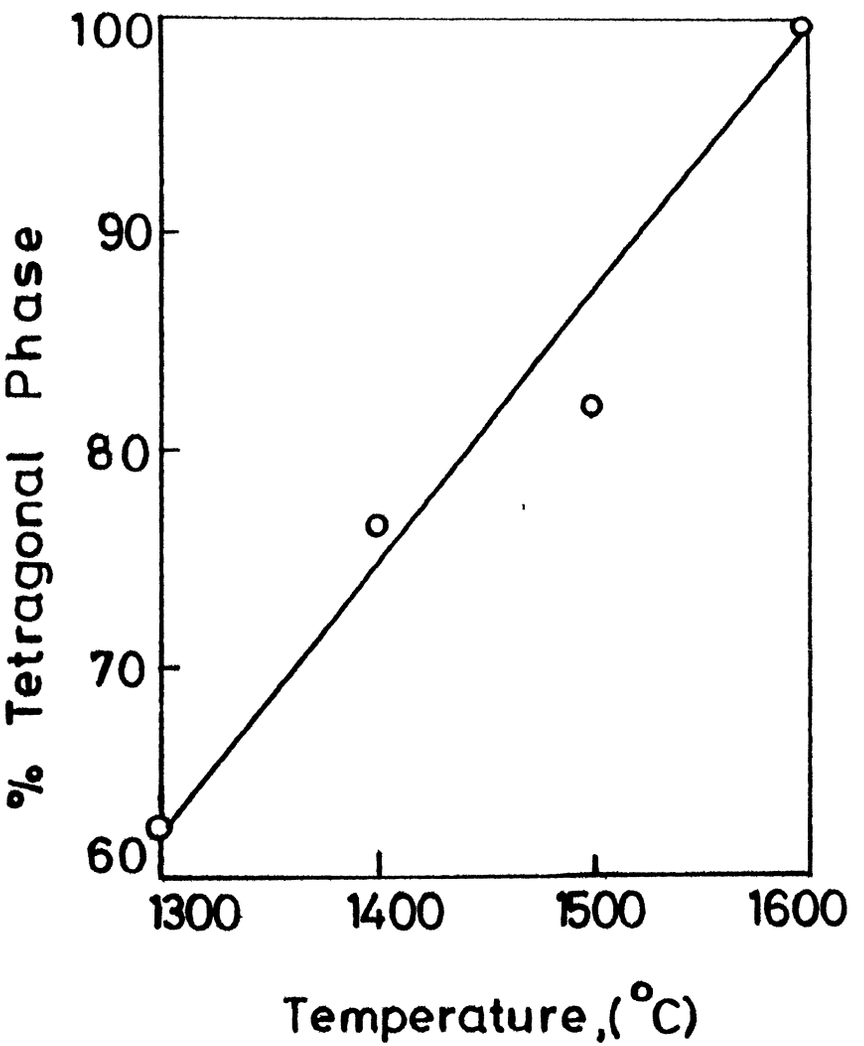

Fig.III.8 Percentage of Retained Tetragonal Phase as a Function of Sintering Temperature for 10 Vol. % TSZ Sample.

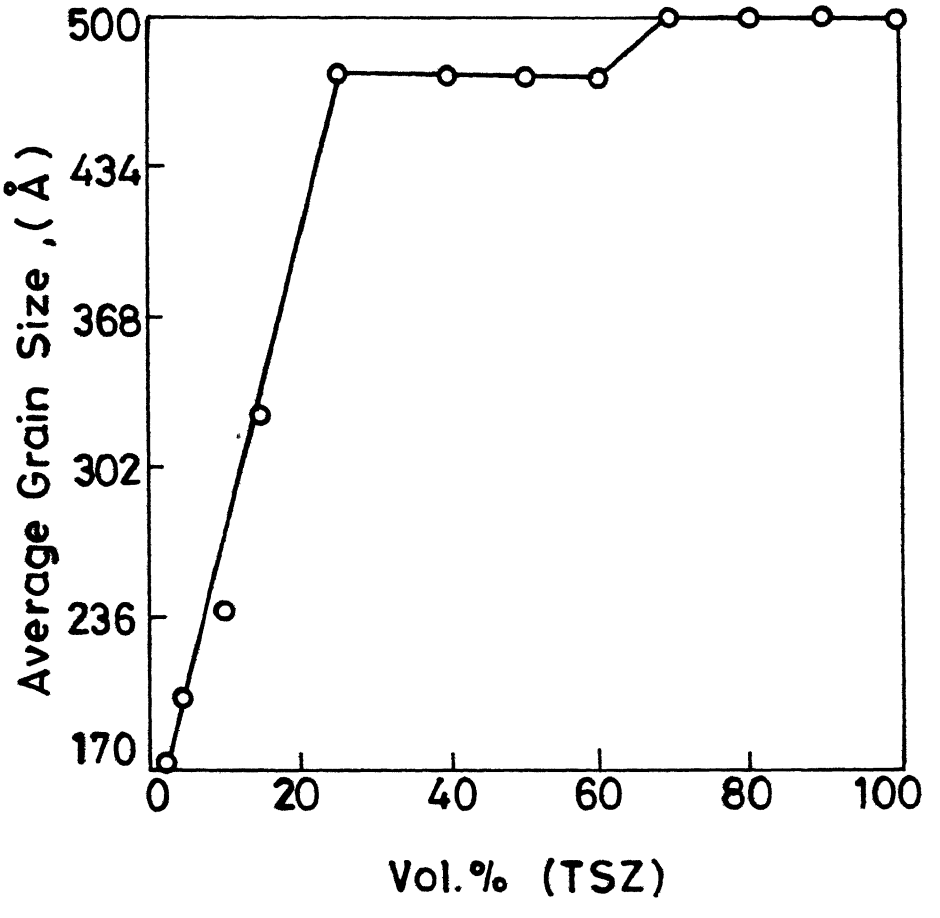

Fig.III.9 TSZ Grain Size as a Function of Vol. % TSZ in ZTA Composites.

phase content with sintering temperature of ZTA composite series, having 10 vol. % TSZ-90 vol% alumina. The figure shows that tetragonal phase retention seems to be in contradiction to the earlier observations in TSZ powder.

Figure III. 10 shows the variation of tetragonal phase retention as a function of vol. % of TSZ in ZTA composites fired at 1600°C for 3 hours. This shows 100 % retention upto almost 50 vol. % TSZ. This also agrees with the observation in Fig. III.8. However, beyond 60 vol. % TSZ, the retention decreases slowly even at 1600°C. It is therefore evident that the variation of retention with TSZ vol. % in ZTA is modified due to presence of alumina, as a consequence of interfacial stresses developed during firing. This situation therefore is very different from that encountered during the investigation of TSZ powder.

3.6 Variation of open, closed and True Porosities with Vol. % of TSZ in ZTA Composites :

Figure III. 11 shows that the open porosity first decreases with vol.% TSZ content and then gradually increases to a maximum, whereas true porosity first increases and then decreases to a minimum. The variation of porosity is predominantly influenced by the closed porosity profile. The initial decrease in open porosity is due to the increase in the fine powder (TSZ) content in a relatively coarse powder (Al_2O_3). The initial increase in closed porosity may be attributed to pore channel closure during sintering. This explaination is supported by the fact that open porosity initially decreases with increase in vol. % TSZ.

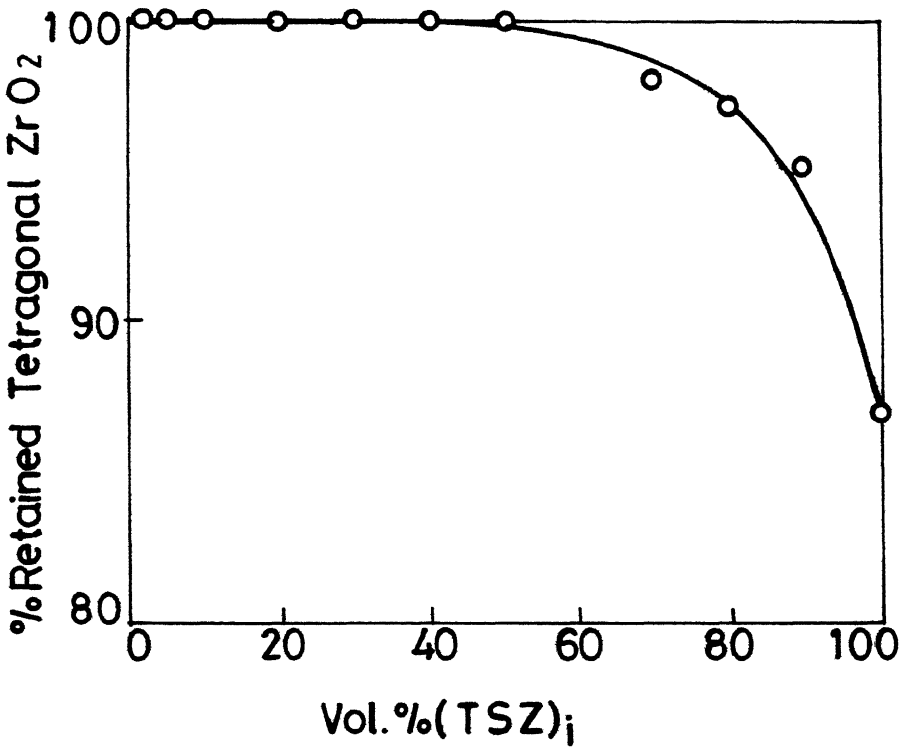

Fig.III.10 Percentage Tetragonal ZrO_2 Retained After Sintering at 1600°C for 3 Hours, as a Function of Volume % Initial TSZ, $[(TSZ)_i]$ in the Green Compact.

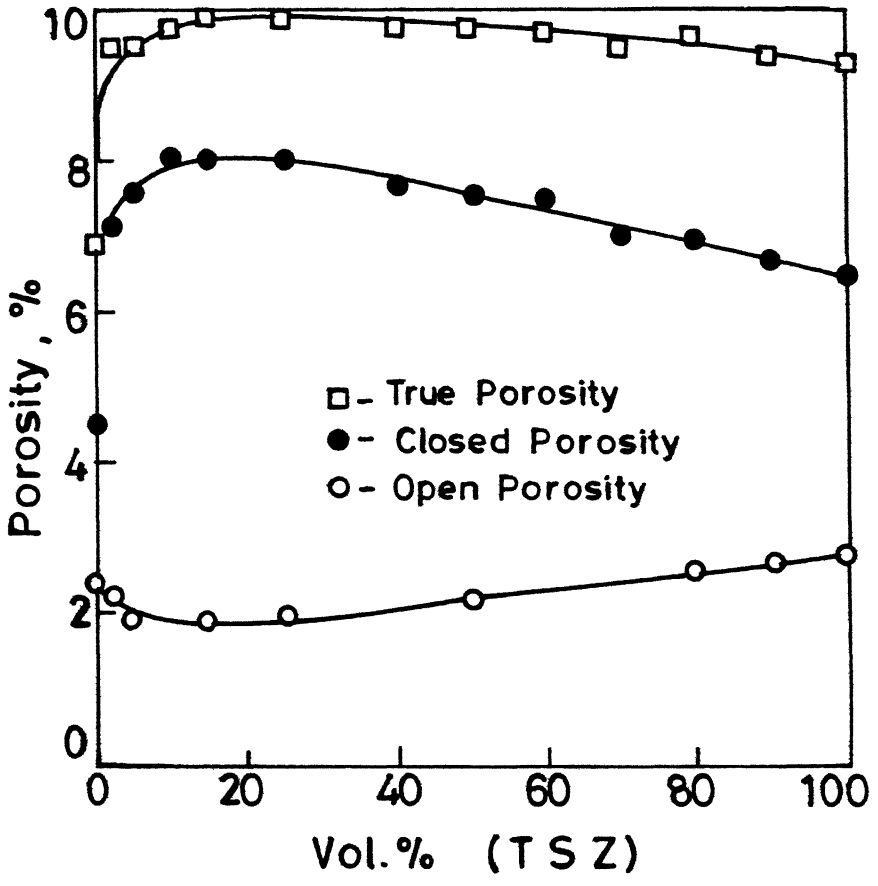

Fig.III.11 Variation of Open, Closed and True Porosities with Vol. % TSZ in ZTA Composites Sintered at 1600 °C for 3 Hours.

3.7 Variation of True and Sintered Density of ZTA Composite with Vol. % of TSZ :

Figure III. 12 shows that both the sintered density and true density increase almost linearly with vol. % TSZ. This is due to a relatively higher density of titania and zirconia as compared to alumina. In addition one notes that the sintered density is closest to the true density at about 30 % TSZ. This is due to efficient filling of pores in the alumina matrix by the relatively finer TSZ powder.

3.8 Variation of Vicker's hardness with Vol. % TSZ in ZTA Composites:

Fig. III. 13 shows that the Vicker's hardness decreases gradually with vol. % TSZ. This is mainly due to the relatively lower hardness of titania and zirconia as compared to alumina. This values of Vickers hardness are higher than those reported by Lange [30] (Maximum hardness = 17.6 GPA).

3.9 Variation of Bend Strength with Vol. % TSZ in ZTA Composites :

A study of Figure III. 14 reveals the following points :

1. Bend strength decreases with vol . % TSZ
2. The rate of decrease of bend strength is more rapid at lower ranges of vol. % TSZ than at higher ranges. This may be attributed to an initial rapid increase in total porosity percentage. The values of bend strength reported here are quite low compared to those reported (350 MPa) by recent worker.[31].

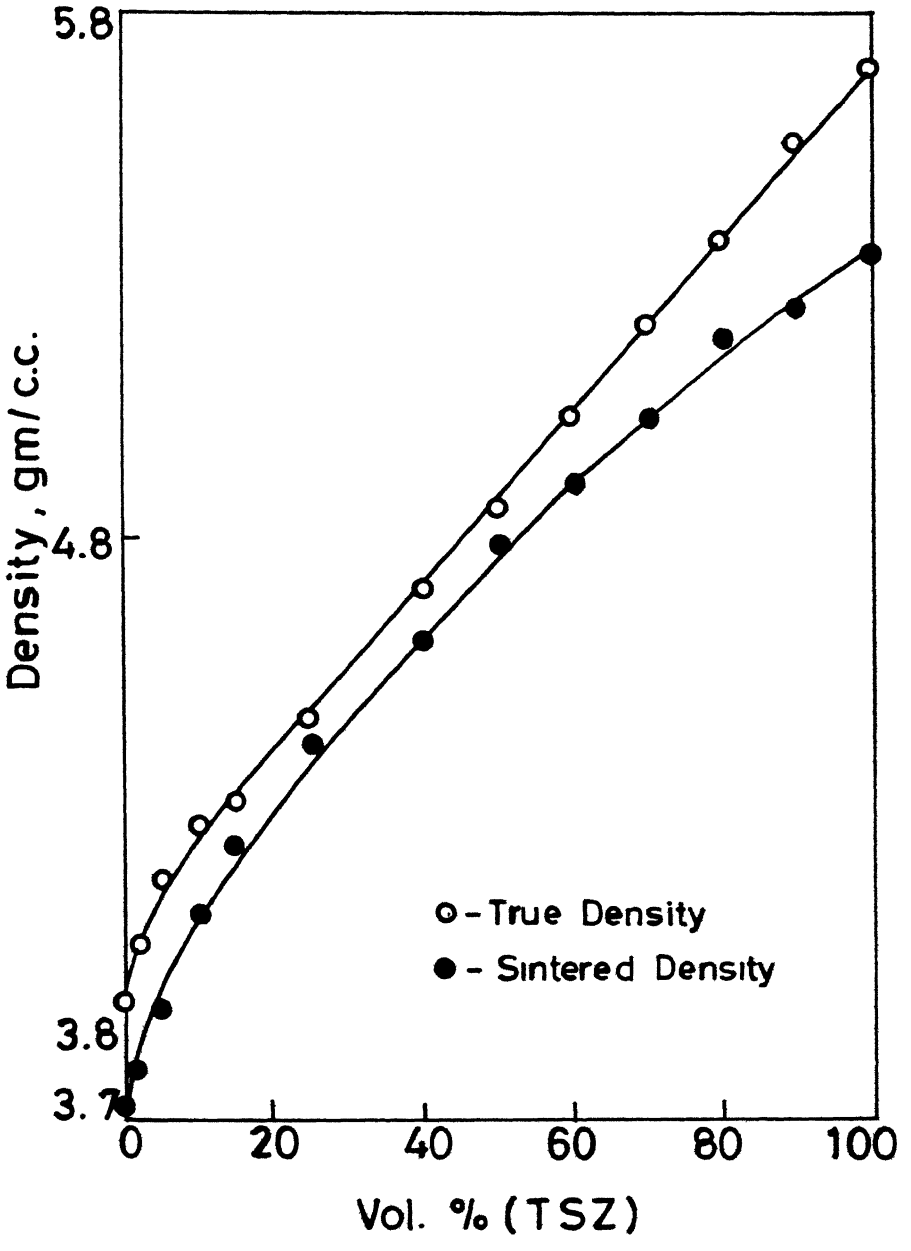

Fig.III.12 Variation of True Density and Sintered Density with Composition for ZTA Composites.

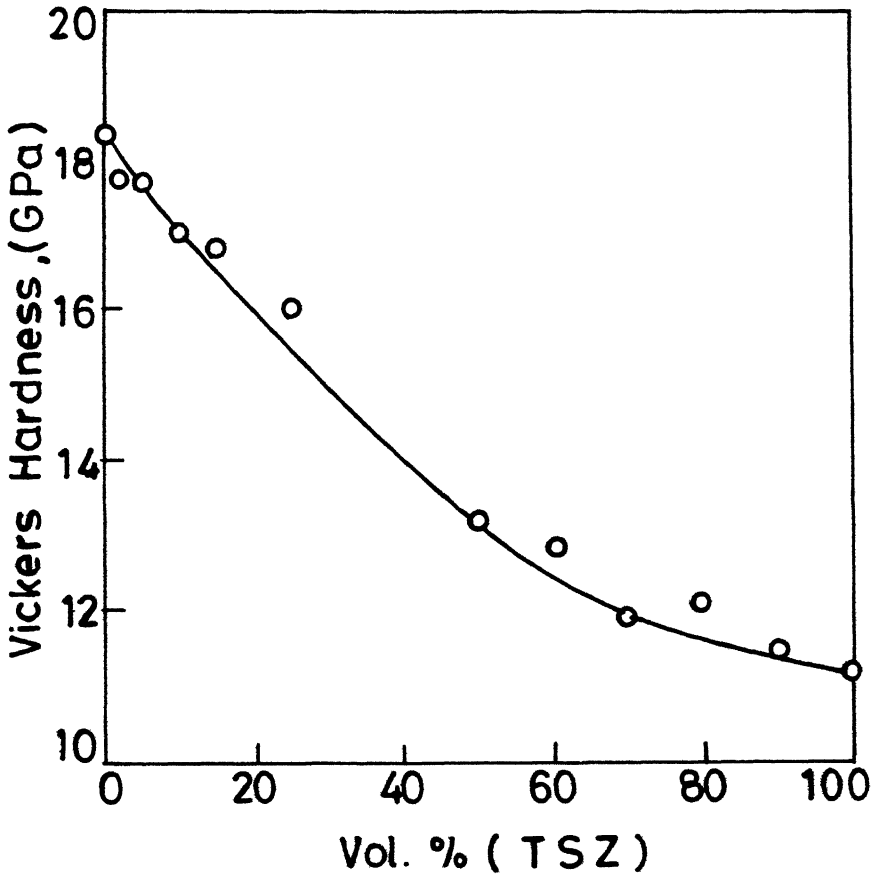

Fig. III.13 Variation of Vickers Hardness with Vol. % TSZ in ZTA Composites.

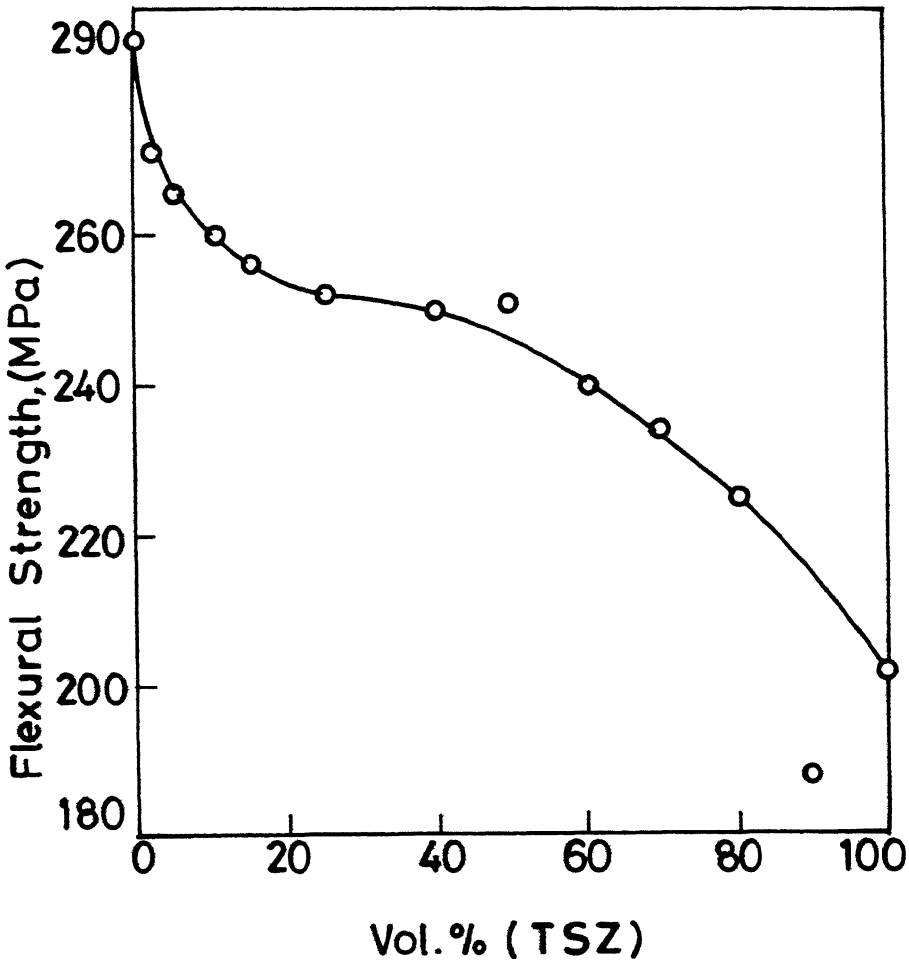

Fig. III.14 Flexural Strength Plotted Against Composition for ZTA Composites.

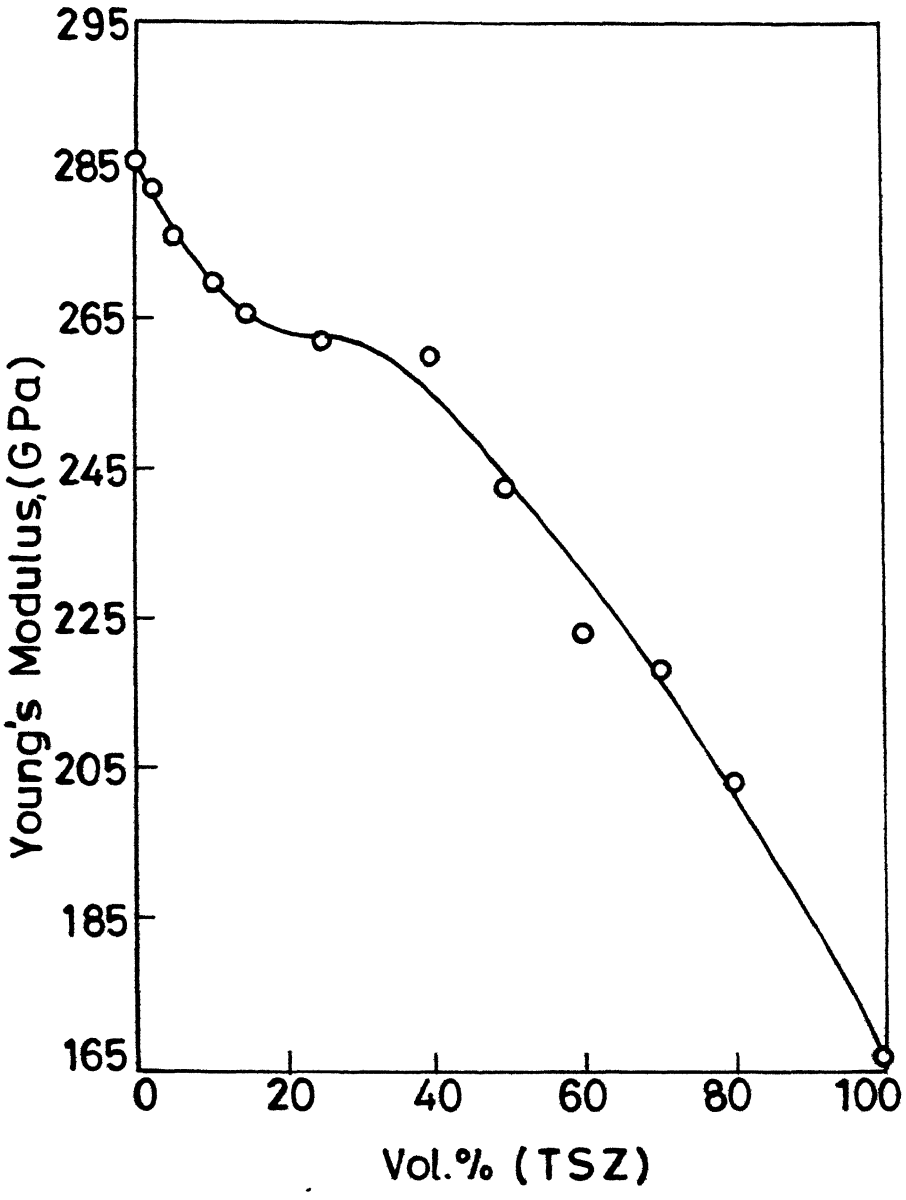

Fig.III.15 Variation of Young's Modulus with Vol.% TSZ in ZTA Composites.

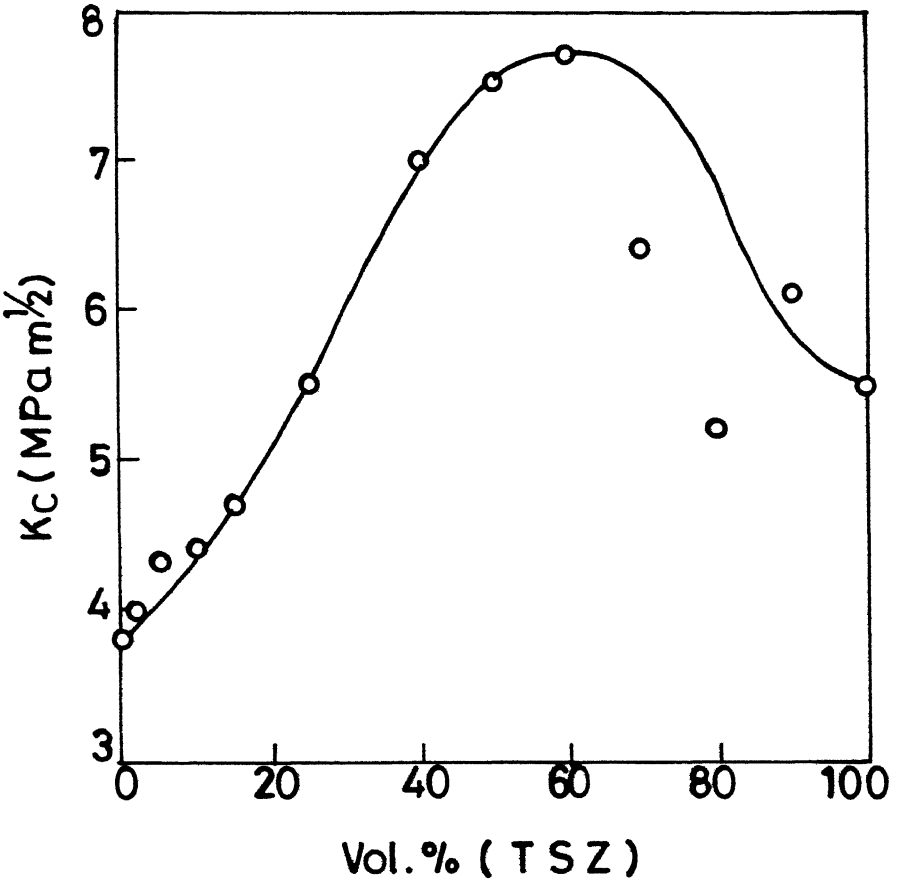

Fig. III.16 Fracture Toughness Plotted Against Vol.% TSZ in ZTA Composites.

3.10 Variation of Young's Modulus with Vol. % TSZ in ZTA Composites :

As shown in Fig. III. 15 Young's modulus variation is similar to the variation of bend strength. The reason for this is same as that given in Section 3.9. However, there is one difference, the decrease in Young's Modulus is more rapid than the decrease in bend strength. This is due to an increase in the central deflection Yc, due to an increase of the more ductile constituent, zirconia. The values reported here are considerably lower than those reported (390 GPa) by recent worker [30].

3.11 Variation of Fracture Toughness with Vol. % TSZ in ZTA Composites :

As shown in Fig. III.16, the fracture toughness, Kc, intially increaes and reaches a maximum of 7.7 MPa-$m^{1/2}$ at about 60 Vol. % of TSZ and gradually declines with further increase in Vol. % TSZ. This existence of a maxima for fracture toughness values may be attributed to almost 100% t phase retention. upto 60 vol. % TSZ. Since 60 vol. % TSZ series contain the maximum amount of TSZ for almost 100 % t-retention, the contribution to fracture toughness is highest. The values reported here, for fracture toughness are quite comparable to those reported (8.13 MPa- $m^{1/2}$) by recent workers [30].

3.12 Microstructure Analysis :

Figure 3.17 shows scanning electron micrographs of the ZTA Composites. From these micrographs, the following points can be noted.

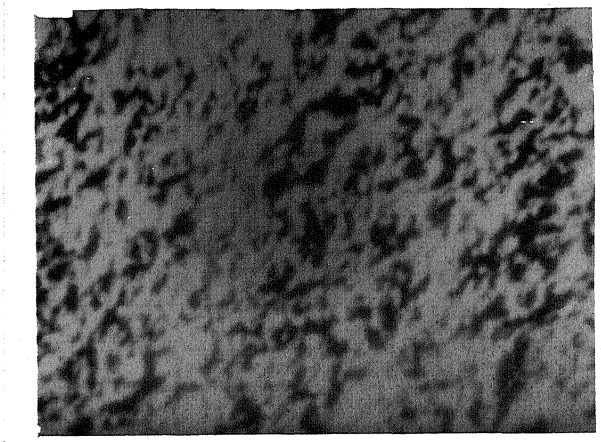

(a)

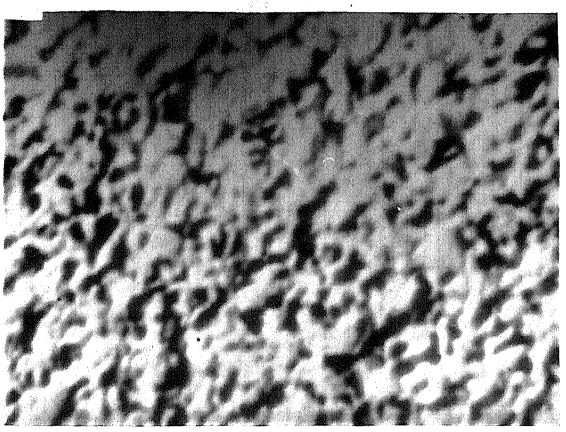

(b)

Fig. III. 17 Scanning Electron Micrographs of (a) Sample No. ZTA 1
(b) Sample No. ZTA 2

(c)

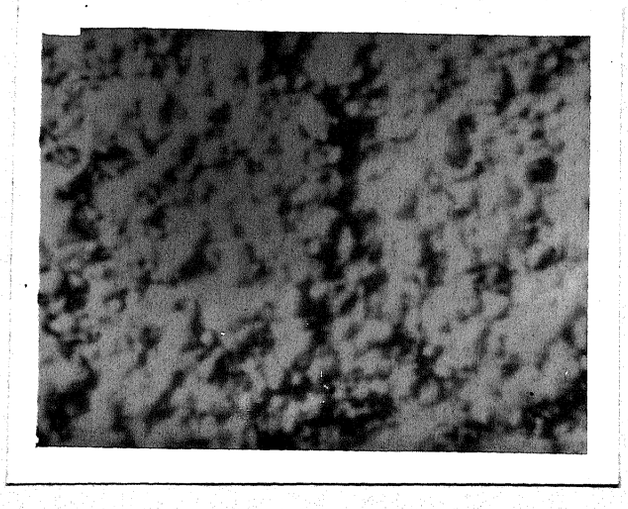

(d)

Fig. III. 17 Scanning Electron Micrographs of (c) Sample No. ZTA 4
(d) Sample No. ZTA 5

1. As the vol. % of TSZ in ZTA increases the grain size increases.
2. As the vol. % TSZ increases total porosity first decreases and then increases rapidly.
3. The extent of agglomeration of the alumina and zirconia particles increases with increasing vol. % TSZ.
4. The grains gradually undergo a change in form, from a dendritic form to a more descrete or uniaxial form, with increasing vol. % TSZ.

CHAPTER - 4

CONCLUSIONS

The following conclusions can be drawn from the present investigation:

1. The particle size analysis shows that precipitation under controlled conditions followed by decomposition, by gradual heating is an excellent method for producing fine powders with greater than 80 % of the particles in the sub-micron range. The average grain size analysis shows that this method also ensures an ultrafine grain size.

2. The abscence of diffraction peaks, corresponding to titania, in the diffraction patterns obtained for TSZ powder, shows that Co-precipitation is a good route for achieving a high degree of homogeniety between the stabilizing and the stabilized constituents.

3. An increase in mole % of TiO_2 in TSZ powders raises the decomposition temperature and lowers the grain size.

4. The stabilizer TiO_2 is highly instrumental in stabilizing the tetragonal phase in zirconia.

5. Almost 100% retention of t-ZrO_2 is possible upto TSZ concentrations as high as 60 vol. % TSZ in ZTA composites sintered at 1600°C for three hours.

6. The sintered density is closest to the true density at around 30 vol. % TSZ in ZTA composites.

7. Vicker's hardness decreases gradually with increasing vol. % TSZ in ZTA composites.

8. Both Flexural strength and Young's modulus decrease with vol. % TSZ, but the decrease in Young's modulus is more rapid.

9. A maxima (7.7 MPa. $m^{1/2}$) exists for the fracture toughness, K_c, at about 60 vol. % TSZ.

SCOPE FOR FURTHER STUDIES :

1. Retention studies as a function of temperature for ZTA composites with larger range of TSZ additions.

2. Development of a relation governing the addition of TSZ and the final grain size in ZTA composites.

3. Determination of the actual role played by Phase-Transformation-Toughening in the improvement of the fracture toughness of ZTA composites, as distinguished from the role of "dispersion of a second phase", "induced microcracking", etc.

GLOSSARY

1. Absolute Hardness : It is the load per unit area of the indentation. The units are same as the units of pressure.

2. Central Deflection: The ma imum deflection in a bend test generally taking place mid-way between the supports where the bending moment is maximum.

3. Closed porosity : It is the ratio of the volume of closed pores to the bulk volume, expressed as a percentage.

4. Flexural Rigidity : It is the product of the Young's modulus and the second moment of area of the specimen. It conveys the same information, about a given specimen, as the Young's modulus does about the material of the specimen.

5. Flexural Strength : It is defined as the maximum bending moment that occurs in the specimen at failure. It is also referred to as the Modulus of Rupture and Bend Strength.

6. Grain : It is that confined region within a material, which has exactly the same lattice structure throughout.

7. Inclusion : It is the particle of the minor phase in a matrix of a major phase.

8. Modulus of Normal Elasticity : It is same as Young's modulus.

9. Open porosity : It is the ratio of the volume of the open pores to the bulk volume, expressed as a percentage.

10. Particle : It is the smallest constituent in a powder which can be physically handled. It is generally an agglomeration of several grains.

11. Radial Crack : It is the crack that originates at the corners of an indentation during a hardness test.

12. Sintered density : It is defined as the ratio of the mass of the material to its apparent solid volume as calculated from its dimensions. It is a term used when considering the density of a porous material.

13. True density : It is defined as the ratio of the mass of the material to its true volume.

14. True Porosity : It is the ratio of the total volume of the open and closed pores to the bulk volume, expressed as a percentage.

15. Ultrafine grain Materials: Materials having an average grain size of 0.1 μm to 10 μm.

REFERENCES

1. R.C. Garvie, " Zirconium Dioxide and some of its Binary Systems'' in'High Temperature Oxides, Part II" ed. Allen M. Alper, (Academic Press, 1970).

2. T.K. Gupta, F.F. Lange and J.H. Bechtold, J. Mater. Sci, 13 (1978) 1964.

3. F.F. Lange, J. Mater. Sci. 17 (1982) 226.

4. Idem, ibid., 17 (1982) 228.

5. Idem, ibid., 17 (1982) 227.

6. Frank H. Brown, Jr., and Pol Duzez, J. Amer. Ceram. Soc. 37 (1954) 132.

7. E. Ryshkewitch, " Oxide Ceramics'' Physical Chemistry and Technology, (Academic Press, 1960).

8. " The Oxide Handbook" ed. G.V. Samsonov (IFI/Plenum 1982).

9. " Ultrafine Grain Ceramics" Proceedings of the 15th Sagamore Army Materials Research Conference (Syracuse University Press, 1970).

10. F.F. Lange, J. Mater. Sci. 17 (1982) 255.

11. A.G. King and W.M. Wheildon, " Ceramics in Machining Processes" (Academic Press, 1966).

12. E.D. Whitney, Powder Metallurgy International 15 (1983) 204.

13. E. Ryshkewitch, " Oxide Ceramics" (J. Springer, Berlin (1984).

14. Jelks Barksdale, "Titanium" Its occurence, Chemistry and Technology, (The Ronald Press Company, New York, 1966).

15. F. Von Bichowsky, Chem. Abs. 27 (1933) 4359.

16. Vogel, "A text Book of Macro and Semi-micro Qualitative Inorganic Analysis". (Longmans, London, 1955)

17. P.A. Evans, R. Stevens and J.G.P. Binner, " Quantitative X-Ray Diffraction Analysis of Polymorphic Mines of Pure Zirconia", Br. Ceram. Trans. J., 83 (1984) 39.

18. Garvie R.C., J. Phys. Chem. 69 (1965) 1238.

19. Vogel, "A Text Book of Quantitative Inorganic Analysis" (Longmans, London, 1955)

20. Geeta Ahuja, "Preparation and Characterization of Alumina-Zirconia Composites", M.Tech. Thesis, Materials Science Program, IIT, Kanpur (1985).

21. Ayal De S. Jayatilaka, "Fracture of Engineering Brittle Materials" (Applied Science Publishers Ltd., London).

22. Br. Ceram. Trans. J., 83 (1984) 43-49.

23. J. Amer Ceram. Soc. 64 (1981) 533.

24. J. Amer. Ceram. Soc., 63 (1980) 574-81.

25. M.V. Swain and J.T. Hagan, J. Phys. B. 11 (1978) 2091-2002.

26. Gunter Petzow, "Metallographic Etching", (American Society for Metals, 1976).

27. George E. Dieter, "Mechanical Metallurgy" (Mc Graw-Hill Book Company, 1986).

28. Lysaght, Vincent E., "Indentation hardness testing" (1949).

29. Claussen et. al. Ceramic Bulletin, 56 (1977) 559.

30. Lange, Journal of Materials Science 17 (1982) 249.